Long-Range Propagation of Plasmon Polaritons in a Thin Metal Film on a One-Dimensional Photonic Crystal Surface

Valery N. Konopsky* and Elena V. Alieva

Institute of Spectroscopy, Russian Academy of Sciences, Troitsk, Moscow Region, 142190, Russia

(Received 1 August 2006; published 22 December 2006)

We present experimental results on ultralong-range surface plasmon polaritons, propagating in a thin metal film on a one-dimensional (1D) photonic crystal surface over a distance of several millimeters. This propagation length is about 2 orders of magnitude higher than the one in the ordinary Kretschmann configuration at the same optical frequency. We show that a long-range surface plasmon polaritons propagation may take place not only in a (quasi)symmetrical scheme, where a thin metal film is located between two media with (approximately) the same refraction index, but also in a scheme where the thin metal film is located between an appropriate 1D photonic crystal and an arbitrary (air, water, etc.) medium. The ultralong-range surface plasmon polaritons are potentially important for biosensors, plasmonics, and other applications.

DOI: 10.1103/PhysRevLett.97.253904 PACS numbers: 42.70.Qs, 73.20.Mf, 78.67.−n, 78.68.+m

Surface plasmon polaritons (SPPs) are bound electromagnetic modes that may exist at a metal-dielectric interface [1]. They are finding ever-widening applications in many fields, ranging from biosensors for the detection of biomolecules and bioreactions on a surface [2] to plasmonics—a young field devoted to guiding optical waves through metal nanostructures [3–5]. One of the main obstacles in developing these fields is an intrinsic damping of the surface plasmon polaritons in the metal and, consequently, a limited propagation distance for the surface plasmon polaritons (about ten micrometers in the optical frequency range). In the early 1980s, it was first predicted [6] and then demonstrated [7] that in thin metal films, imbedded between two identical dielectrics [Fig. 1(a)], a long-range surface plasmon-polariton (LRSPP) mode may appear as a result of a coupling between SPPs from both film interfaces. Compared with conventional SPPs, LRSPPs have higher surface electric field strengths, longer propagation lengths, and, consequently, narrower angular resonance curves. Several attempts have been made to exploit LRSPPs instead of SPPs in typical SPP applications, such as surface plasmon resonance biosensors [8,9] and surface-plasmon-enhanced high-harmonic generation [10]. A drawback of LRSPP applications is the more complicated scheme required for LRSPP excitation [Fig. 1(b)], compared to the ordinary Kretschmann scheme for SPP excitation, due to the need for a matching layer (usually a matching fluid) to match the refraction indexes (RIs) of the media on both sides of the film. For many media with a low RI n_e under investigation (e.g., water), this approach is hardly applicable. It becomes impractical for $n_e \simeq 1$ (air), since a freely suspended thin film is needed in this case.

In this Letter we describe LRSPPs that may propagate at metal-air, metal-water, etc., interfaces and have propagation lengths about 2 orders of magnitude higher than those in the ordinary Kretschmann configuration at the same optical frequency. The above objective is attained by using an appropriate 1D photonic crystal instead of the matching layer, as shown in Fig. 1(c). Here we show that this scheme may support even more long-range SPPs (i.e., ultralong-range SPPs) than the usual symmetrical scheme for LRSPPs.

First, it is important to note that the principal reason for long-range plasmon propagation is the presence of a minimum electric field strength in the thin metal film as the result of destructive interference by SPPs from both film interfaces. This minimum coincides with the zero of the main, tangential component E_y of the electric field in the metal. We find general conditions for existing of the tangential electric field zero in the thin metal film. In this Letter, let a p-polarized electromagnetic field be an incident on a metal film with complex RI n_M and thickness d_M at an angle θ_0 from an internal medium with RI n_0. Hereafter, we will use a numerical aperture $\rho = n_0 \sin(\theta_0)$ as an angle variable instead of the angles θ_j at

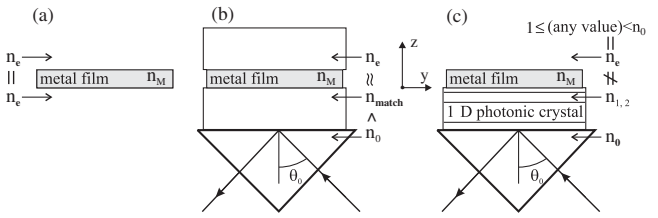

FIG. 1. Structures supporting long-range surface plasmon polaritons propagation. (a) A symmetric scheme with identical dielectrics on both sides of the thin metal film. (b) A Kretschmann-like quasisymmetric scheme for LRSPP excitation by frustrated TIR on the prism. For the drawbacks of this scheme, refer to the text. (c) The presented scheme—a thin metal film on a 1D photonic crystal. The external medium may have any RI in the range $1 \leq n_e < n_0$, subject to an appropriate choice of 1D photonic crystal structure.

different layers. This will be a unified angle variable for all layers since, according to Snell's law, $\rho = n_0 \sin(\theta_0) = n_j \sin(\theta_j)$, for any layer j. We will consider the case $\rho \geq n_e$, which is the total internal reflection from the external medium with RI n_e. Assuming that $d_m \ll \lambda$, $|n_M| > n_e$ and looking for the zero minimum of the electric field modulus $|E_y|$ in the thin film, one can find that the zero minimum takes place at the incident angle

$$\rho_\alpha = n_e + 2\alpha^2 \frac{n_e^3 d_M^2 \pi^2}{\lambda^2}, \tag{1}$$

where $\alpha = (d_M - z_0)/d_M$ is the coordinate of the zero minimum z_0 in terms of film thickness d_M. When $z_0 = 0$ ($\alpha = 1$), and the angle of incidence is $\rho = \rho_1$, the zero minimum of the electric field modulus $|E_y|$ takes place at an internal border of the film. When $z_0 = d_M/2$ ($\alpha = 1/2$), the zero minimum occurs at $\rho = \rho_{1/2}$ in the center of the film. When $z_0 \to d_M$ ($\alpha \to 0$), the zero minimum of $|E_y|$ is located at an external border of the film, and this takes place at ρ_0 infinitesimally close to n_e (i.e., near the angle of total internal reflection).

So the electric field modulus $|E_y|$ has a minimum equal to zero when the p-polarized electromagnetic wave incident on the thin metal film is in the angular range from ρ_1 to ρ_0. In this case, the point where $|E_y| = 0$ is changed from the internal to external border of the film.

Now we look for electromagnetic surface modes which have a wave vector in the range: $k = [\frac{\omega}{c}\rho_1 \ldots \frac{\omega}{c}\rho_0]$. One may expect that such modes will be long-range propagated surface modes, since they may be excited by the p-polarized waves incident on the film in angular range $\rho = [\rho_1 \ldots \rho_0]$, and these modes have the zero minimum of $|E_y|$ inside the metal film.

One example of such a mode is already familiar to readers—the LRSPP in a thin film embedded between two identical dielectrics [Fig. 1(a)]. It is known that the dispersion curve of SPPs splits as a result of a coupling between SPPs from both film interfaces, and the LRSPP wave vector shifts (at a given frequency) to a light curve. The value of the LRSPP wave vector is $k \simeq \frac{\omega}{c}\rho_{1/2}$ [11], where $\rho_{1/2}$ is given by (1) at $\alpha = 1/2$, and the zero minimum of $|E_y|$ is always located in the center of the film.

Here we present another example of electromagnetic surface modes that can propagate along thin metal films and have a wave vector in the range of $k = [\frac{\omega}{c}\rho_1 \ldots \frac{\omega}{c}\rho_0]$—optical surface waves on the 1D photonic crystal surface. Photonic crystals (PCs) are materials that possess a periodic modulation of their refraction index on the scale of the wavelength of light [12]. Such materials can exhibit photonic band gaps that are very much like the electronic band gaps for electron waves traveling in the periodic potential of the crystal. In both cases, frequency intervals exist where the wave propagation is forbidden. This analogy may be extended [13] to include surface levels, which can exist in band gaps of electronic crystals. In PCs it will be the optical surface wave, which dispersion curve is located inside the photonic band gap.

The 1D PC is a simple periodic multilayer stack. Optical surface modes in 1D PCs were studied in the 1970s by the Yariv group, both theoretically [14] and experimentally [15]. Twenty years later, Robertson *et al.* experimentally studied the excitation of optical surface waves in a Kretschmann-like configuration [16,17]. All of these studies dealt with s-polarized (i.e., transverse electric, TE) optical surface waves. We will exploit p-polarized (i.e., transverse magnetic, TM) optical surface waves on the 1D PC ended by the thin metal film.

The 1D PC structure for our experiments [18] was deduced in the following way: (a) approximated parameters of the 1D PC were calculated (at given λ, n_1, n_2, n_M, $d_M \sim 5$ nm, and $\rho \sim n_e$) from a dispersion relation for the TM optical surface mode in the thin metal film on *semi-infinite* 1D PC. Then (b) obtained thicknesses d_1, d_2 were numerically optimized for real *finite* 1D PC on the given substrate.

The dispersion relation for the TM optical surface mode in the film on the *semi-infinite* 1D PC was derived in the regular way: the tangential components of electric and magnetic fields were matched at both interfaces of the film with the RI n_3 and the thickness d_3. The field amplitude in the external medium above the film is described by a decaying exponential, and by a standing wave with an exponentially decaying envelope e^{Kz} in the 1D PC below the film. We obtain the next dispersion relation for the TM optical surface mode:

$$\frac{n_3^2[k_{3z} n_e^2 + q_e n_3^2 \tan(k_{3z} d_3)]}{k_{3z}[q_e n_3^2 - k_{3z} n_e^2 \tan(k_{3z} d_3)]} = -\frac{i n_1^2 (B - e^{-iK\Lambda} + A_1)}{k_{1z}(B + e^{-iK\Lambda} - A_1)}, \tag{2}$$

where $k_{iz} = (n_i^2 k_0^2 - k_y^2)^{1/2}$, $i = 1 \ldots 3$, $q_e = (k_y^2 - n_e^2 k_0^2)^{1/2}$, $k_0 = \omega/c$, $k_y = k_0 \rho$, $\Lambda = d_1 + d_2$. Parameters of the semi-infinite 1D PC from the right-hand side of Eq. (2) are

$$e^{-iK\Lambda} = \frac{1}{2}\{A_1 + A_2 - [(A_1 + A_2)^2 - 4]^{1/2}\},$$

$$A_{\frac{1}{2}} = e^{\mp i k_{1z} d_1}\left[\cos(k_{2z} d_2) \mp \frac{1}{2} i Z_{1/2} \sin(k_{2z} d_2)\right],$$

$$Z_{1/2} = \left(\frac{{n_2}^2 k_{1z}}{{n_1}^2 k_{2z}} + \frac{{n_1}^2 k_{2z}}{{n_2}^2 k_{1z}}\right),$$

$$B = -\frac{1}{2} i e^{i k_{1z} d_1}\left(\frac{{n_2}^2 k_{1z}}{{n_1}^2 k_{2z}} - \frac{{n_1}^2 k_{2z}}{{n_2}^2 k_{1z}}\right)\sin(k_{2z} d_2).$$

The calculated dispersion of our *finite* test 1D PC structure is presented in Fig. 2 as the logarithm of optical field enhancement in the external medium near the structure. We have prepared [20] the test 1D PC structure and measured angles of the SPP excitation at different wavelengths. Good

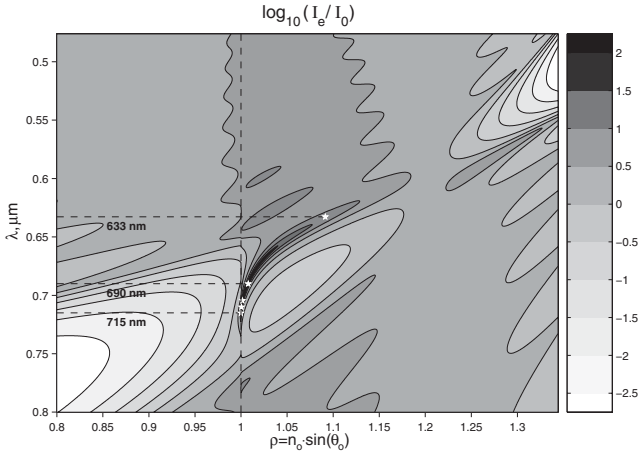

FIG. 2. The calculated dispersion of the test 1D photonic crystal structure and measured experimental points (white pentagrams) at different wavelengths. The photonic band gap is clearly seen as light areas with an enhancement much less than 1. The photonic band gap vanishes near Brewster's angle ($\rho_{\mathrm{Br}} \simeq 1.2$ in this system), where no reflection of the TM wave takes place from the SiO_2/Ta_2O_5 interface. The optical surface mode is seen as a dark curve with an enhancement more than 100 inside the band gap. The white pentagrams are experimental points measured at $\lambda = 633$ nm (He-Ne laser), $\lambda = 690$ nm (diode laser), and $\lambda = 704.5$ nm, $\lambda = 710.1$ nm, $\lambda = 715.25$ nm (Ti-sapphire laser).

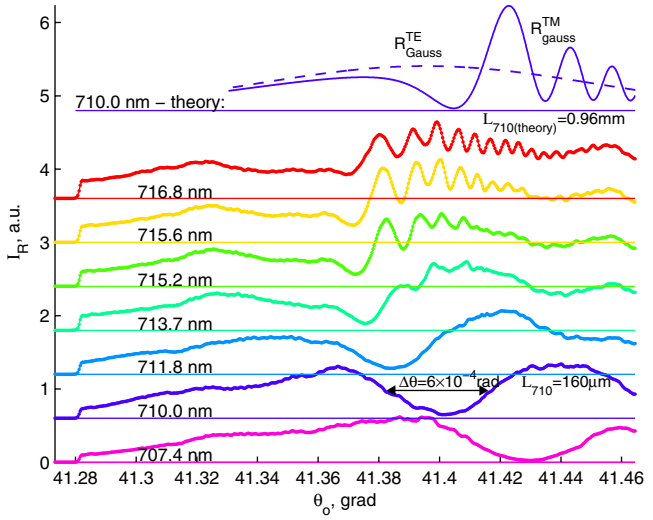

FIG. 3 (color online). Angular resonance curves at different wavelengths. Each curve is up-shifted by 0.6 a.u. from the previous one for good visibility. The diode array was shaded at $\theta_0 \leq 41.28$ to mark the zero level. The interference near the plasmon resonance curves at $\lambda > 714$ nm is a new distinguishing feature of ultralong-range SPPs in the Kretschmann-like configuration (see text for details).

correspondence is seen between experimental points [21] and the calculated dispersion curve of the surface mode. Figure 2 illustrates that the optical surface mode dispersion curve approaches the line of the total internal reflection (TIR) ($\rho_{\mathrm{TIR}} \equiv n_e = 1$) at wavelengths in the range of $\lambda \sim [704 \ldots 718]$ nm. Therefore, at these wavelengths we can excite the SPP at $\rho \rightarrow n_e$ and expect it to be LRSPP. At $\rho = \rho_{1/2}$ (in our structure it takes place at $\lambda \simeq 711$ nm), the zero minimum of $|E_y|$ occurs in the center of the 5 nm gold film. Moreover, at $\lambda \rightarrow 718$ nm $\rho = \rho_0 \rightarrow n_e$ and we can excite LRSPPs with $|E_y| = 0$ at the external interface of the gold film. It may be shown that the intrinsic extinction of LRSPPs decreased and the propagation length increased when α from Eq. (1) goes to zero. Therefore, contrary to intuitive expectations, modes with $\rho = \rho_0 \rightarrow n_e$ ($|E_y| = 0$ at the external interface of the film) are more long-range propagated than the mode with $\rho = \rho_{1/2}$ ($|E_y| = 0$ in the center of the film). To confirm this statement experimentally we have recorded the angular resonance curves of LRSPPs at different wavelengths.

Angular resonance curves [22] are presented in Fig. 3. One can see that the angular curve width at $\lambda = 710$ nm is $\Delta\theta = 6 \times 10^{-4}$ rad, which corresponds to the SPP propagation length (length of $1/e$ intensity decreasing) $L_{710} \simeq 160$ μm. This is about 20 times higher than the SPP propagation in the ordinary Kretschmann configuration at optimal film thickness at the same wavelength ($L_{\mathrm{SPP}} \simeq 8$ μm). As we increase the wavelength, the resonance angle shifts to the TIR angle [$\theta_0^{\mathrm{TIR}} = \arcsin(1/n_0) \simeq 41.37$ grad] and the resonance curve width decreases (hence the propagation length increases). For instance, at $\lambda = 715.2$ nm, the propagation length is estimated to be $L_{715} \simeq 0.8$ mm, which is about 2 orders of magnitude higher than L_{SPP} in the ordinary Kretschmann scheme. Moreover, a new distinguishing feature of ultralong-range SPPs in the Kretschmann-like configuration appears: interference near the plasmon resonance curve. This interference cannot be theoretically predicted from Fresnel-based calculations of reflection curves since the incident field is approximated as an infinite flat front in these calculations, and the limited propagation of SPPs is compared with infinity. However, describing the reflection of a focused restricted Gaussian laser beam, the interference appears when SPP propagation length becomes much more than a waist of the incident Gaussian beam. One can obtain a qualitative picture of this phenomenon considering destructive interference of two collinear Gaussian beams when one of them (the reflected beam in our case) has much less waist than another (the beam from LRSPPs reradiated back to the prism). The waist difference leads to the difference in Rayleigh ranges and to the difference in wave front curvatures of these beams at some distances. Intersections of constant phase fronts of these beams produce the interference. Theoretical curves presented in Fig. 3 give the exact quantitative description of the Gaussian beam reflection from our structure. Note that the experimental propagation length of LRSPP is 6 times less than the theoretical one due to roughness scattering of LRSPP to a free-propagated light. The measured propaga-

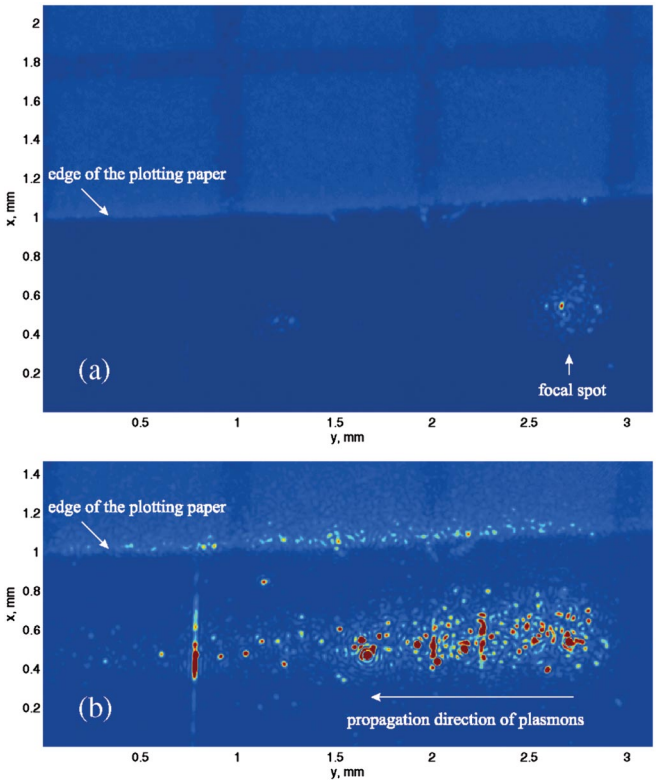

FIG. 4 (color). Photographs of the focused laser beam near the SPP resonance: (a) slightly off resonance and (b) in resonance. Plotting paper is placed near the laser focus on the film to designate the scale. The photographs were made from the external side of the film [from the upper side of Fig. 1(c)]. Ideally, no light must be seen from this side since total internal reflection of all light occurs. However, in actual practice, light is scattered on imperfections, which are always present on real surfaces, and this scattered light may be detected from the external side.

tion length, consequently, is determined by the plasmon-photon scattering rather than by the internal damping.

When the LRSPP propagation length reaches large values, the trace of LRSPPs may easily be seen by the naked eye. Figure 4 presents photographs of the laser beam focused using a lens with focal length $f = 435$ mm, both out of resonance [Fig. 4(a)] and in resonance [Fig. 4(b)]. One can see in Fig. 4(b), as different scratches and roughness are visualized by the plasmon field while the SPPs travel the several-millimeter distance.

In conclusion, we have used the unique wavelength tunable properties of 1D photonic crystals for the excitation of SPPs along a thin metal film in that wave vector range where they become ultralong-range SPPs and may exist in an asymmetric configuration.

This work was partly supported by the European Network of Excellence, No. NMP3-CT-2005-515703-2. The authors thank V. O. Kompanets for technical assistance in work with the Ti-sapphire laser.

*Electronic address: konopsky@isan.troitsk.ru

[1] H. Raether, *Surface Plasmons* (Springer, New York, 1988).
[2] J. Homola, S. S. Yee, and G. Gauglitz, Sensors and Actuators B (Chemical) **54**, 3 (1999).
[3] E. Ozbay, Science **311**, 189 (2006).
[4] M. Quinten, A. Leitner, J. R. Krenn, and F. R. Aussenegg, Opt. Lett. **23**, 1331 (1998).
[5] S. I. Bozhevolnyi, V. S. Volkov, E. Devaux, J.-Y. Laluet, and T. W. Ebbesen, Nature (London) **440**, 508 (2006).
[6] D. Sarid, Phys. Rev. Lett. **47**, 1927 (1981).
[7] A. E. Craig, G. A. Olson, and D. Sarid, Opt. Lett. **8**, 380 (1983).
[8] G. Nenninger, P. Tobiška, J. Homola, and S. Yee, Sensors and Actuators B (Chemical) **74**, 145 (2001).
[9] A. W. Wark, H. J. Lee, and R. M. Corn, Anal. Chem. **77**, 3904 (2005).
[10] H. J. Simon, Y. Wang, L.-B.Zhou, and Z. Chen, Opt. Lett. **17**, 1268 (1992).
[11] F. Yang, J. R. Sambles, and G. W. Bradberry, Phys. Rev. B **44**, 5855 (1991).
[12] E. Yablonovitch, J. Opt. Soc. Am. B **10**, 283 (1993).
[13] D. Kossel, J. Opt. Soc. Am. **56**, 1434 (1966).
[14] P. Yeh, A. Yariv, and C.-S. Hong, J. Opt. Soc. Am. **67**, 423 (1977).
[15] P. Yeh, A. Yariv, and A. Y. Cho, Appl. Phys. Lett. **32**, 104 (1978).
[16] W. M. Robertson and M. S. May, Appl. Phys. Lett. **74**, 1800 (1999).
[17] W. M. Robertson, J. Lightwave Technol. **17**, 2013 (1999).
[18] The following 1D PC structure was used in experiments: substrate/$(HL)^{14}H'M$/air, where H is a Ta_2O_5 layer with thickness $d_2 = 100.0$ nm, L is a SiO_2 layer with $d_1 = 155.7$ nm, H' is a Ta_2O_5 layer with $d_2' = 98.4$ nm, and M is a gold layer with $d_3 = d_M = 5$ nm. The prism and substrate were made from BK-7 glass. The RIs of the substrate, Ta_2O_5, SiO_2, and Au at $\lambda = 710$ nm, were $n_0 = 1.513$, $n_2 = 2.13$, $n_1 = 1.45$, and $n_3 = n_M = 0.2 + i4.14$, correspondingly. The RIs at other wavelengths were derived using dispersion data presented by Palik [19].
[19] E. D. Palik, *Handbook of Optical Constants of Solids* (Academic, New York, 1985).
[20] The Ta_2O_5/SiO_2 multilayer was deposited by ion sputtering. The gold film was deposited by ion-assisted rf-frequency diode sputtering. The specific electrical resistance of our sputtered gold film was measured to be 16.3 $\mu\Omega$ cm, which is 7.4 times higher than the specific resistance (2.2 $\mu\Omega$ cm) of bulk gold.
[21] The excitation angles of the optical surface waves, indicated as white pentagrams in Fig. 2, were experimentally measured with an angular accuracy of $\pm 1'$ by parallel laser beam at specified laser wavelengths.
[22] The angular resonance curves in Fig. 3 were measured by focusing the laser beam (with diameter $D \simeq 2$ mm) on the structure, in Kretschmann-like geometry, with the objective of a focal length of $f = 220$ mm, and detecting the intensity distribution of reflected light with a 512-pixels Hamamatsu photodiode array placed 1980 mm apart from the structure.